Influence of a Toroidal Field on Plasma Confined in a Toroidal Octupole

D. E. LENCIONI, J. W. POUKEY*, J. A. SCHMIDT, J. C. SPROTT, AND C. W. ERICKSON†
University of Wisconsin, Madison, Wisconsin

(Received 24 July 1967; final manuscript received 10 January 1968)

A toroidal magnetic field B_θ of up to 360 G was added to the Wisconsin toroidal octupole producing a stellarator-like field with a large rotational transform and large shear. The influence of this B_θ on plasma injection, transport, density distribution, lifetime, and electric-field fluctuations was studied. Injection and transport were not inhibited by B_θ and proceeded in much the same way as for $B_\theta = 0$. The density distribution after filling was unchanged and remained peaked slightly off the separatrix toward the hoops. The lifetime was smaller with E_θ, but was still consistent with expected losses to the hoop supports. In the originally V'' unstable region outside the last stable field line, the amplitude of the electric field fluctuations decreased when B_θ was added, but in the interior of the plasma, the fluctuations increased monotonically with B_θ. In the plasma interior the maximum diffusion coefficient derived from the fluctuations increased from $10^{-4}\,D_{\text{Bohm}}$ to $10^{-2}\,D_{\text{Bohm}}$ as B_θ was increased from zero to 140 G, but the observed lifetime, limited by hoop supports, was always $\sim 10\,\tau_{\text{Bohm}}$. Large potential deviations which were affected by magnetic field perturbations occurred in the region of zero average shear. Large external-field perturbations were added with no effect on the lifetime. Fluctuations associated with stable inverted density gradients were reduced or eliminated by B_θ.

I. INTRODUCTION

Circumferential currents flowing in a toroidal multipole conductor system produced a multipole field for containing plasma. The magnetic field was poloidal, i.e., there was no circumferential component, and thus the field lines were closed around the embedded conductors.[1] These toroidal multipoles can be designed to have deep average minimum field for strong magnetohydrodynamic stability.[2] The earliest experiments, conducted on the Wisconsin toroidal octupole, showed that indeed there was stability and that the containment time was consistent with losses to the conductor supports and probes.[1,3-5] Also, any fluctuations observed in the main body of the plasma were minute, in the sense that within the plasma the diffusion coefficient derived from them was $\sim 10^4$ times smaller than the Bohm value.[6] This should be compared with the fluctuations observed in other closed systems. For example, in some stellarators having plasmas of similar density and temperature, the Bohm value for diffusion was obtained.[7]

Other containment experiments, also providing quiescent plasmas, with poloidal fields were later made. For example, Ohkawa carried out a similar octupole experiment,[8] while von Gierke used a cesium plasma in a toroidal octupole and found diffusion loss $\approx 1\%$ of Bohm loss.[9] Recently Voorhies reported tests on a small toroidal multipole.[10]

If a toroidal field is superimposed on the poloidal field, the lines of force in general no longer close but they spiral and map out an entire flux surface. Furthermore, the toroidal field now gives the system shear. Berkl reported that a plasma was produced under carefully adjusted conditions in the Munich cesium stellarator containing both a poloidal and toroidal field which showed a loss much smaller than the Bohm loss.[11]

In the Wisconsin experiment flexibility was obtained by conducting identical experiments with and without the toroidal (B_θ) field. Some of the questions of how this added circumferential field influenced the contained plasma are answered by the experimental results described here. These results, with and without B_θ, will be presented side by side for comparison. The result of a similar experiment was reported by Yoshikawa.[12]

* Present address: Sandia Corporation, Albuquerque, New Mexico.
† Present address: Institute for Plasma Physics, Garching bei München, Germany.

[1] D. W. Kerst, R. A. Dory, W. E. Wilson, D. M. Meade, and C. W. Erickson, Phys. Rev. Letters **15**, 396 (1965).
[2] T. Ohkawa and D. W. Kerst, Phys. Rev. Letters **7**, 41 (1961); Nuovo Cimento **22**, 784 (1961).
[3] W. E. Wilson and D. M. Meade, Bull. Am. Phys. Soc. **9**, 495 (1964).
[4] W. E. Wilson and D. M. Meade, Bull. Am. Phys. Soc. **9**, 532 (1964).
[5] R. A. Dory, D. W. Kerst, D. M. Meade, W. E. Wilson, and C. W. Erickson, Phys. Fluids **9**, 997 (1966).
[6] D. M. Meade, Phys. Rev. Letters **17**, 677 (1966).
[7] W. Stodiek, D. J. Grove, and J. O. Kessler, in *Plasma Physics and Controlled Nuclear Fusion Research* (International Atomic Energy Agency, Vienna, 1966), Vol. II, p. 687.
[8] T. Ohkawa, A. A. Schupp, Jr., M. Yoshikawa, and H. G. Voorhies, *Plasma Physics and Controlled Nuclear Fusion Research* (International Atomic Energy Agency, Vienna, 1966), Vol. II, p. 531.
[9] D. Eckhartt, G. von Gierke, and G. Grieger, in *Plasma Physics and Controlled Nuclear Fusion Research* (International Atomic Energy Agency, Vienna, 1966), Vol. II, p. 719.
[10] H. G. Voorhies and T. Ohkawa, Bull. Am. Phys. Soc. **12**, 789 (1967).
[11] E. Berkl, D. Eckhartt, G. von Gierke, and G. Grieger, Phys. Rev. Letters **17**, 906 (1966).
[12] M. Yoshikawa, T. Ohkawa, and A. A. Schupp, Jr., Bull. Am. Phys. Soc. **12**, 789 (1967).

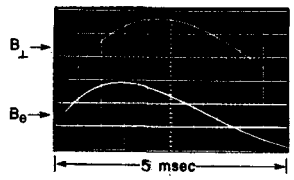

FIG. 1. Oscilloscope traces of the poloidal ($B_\perp$) and toroidal (B_θ) magnetic fields. At the outside wall midplane $B_\perp$ reaches a maximum of 1 kG and B_θ reaches a maximum of 250 G.

The toroidal field was produced simply by insulating the lid of the conducting multipole vacuum tank at its outer circumferential flange and by energizing 32 distributed terminals at this gap so that the whole box formed a one-turn toroidal coil.

The two components of the field are shown in Fig. 1. The peak in the poloidal and toroidal fields at the midplane and outer wall are, respectively, 1 kG and 250 G.

An effectively collisionless hydrogen plasma was used for the experiment with an ion temperature of $\approx$40 eV, an electron temperature of $\approx$10 eV, and density of $\approx 10^9$ cm^{-3}. The above field strengths and proton energy give 7.3 to 15.2 gyroradii across the stable plasma region.

II. FIELD TOPOLOGY

The component of **B** in a θ = const plane ($\mathbf{B}_\perp$) is related to its corresponding flux function (ψ) by

$$\mathbf{B}_\perp = (\hat{\theta} \times \nabla\psi)/2\pi R,$$

where R is the distance from the toroid's major axis and θ is the angular coordinate around the toroid. It follows that lines of constant ψ are also $\mathbf{B}_\perp$ lines and that the total flux between two ψ surfaces, ψ_1 and ψ_2 is $(\psi_1 - \psi_2)$, where a ψ surface is obtained from a ψ line by one revolution around the toroid's major axis. A computer-obtained, design-run plot[13] of the ψ lines is given in Fig. 2.

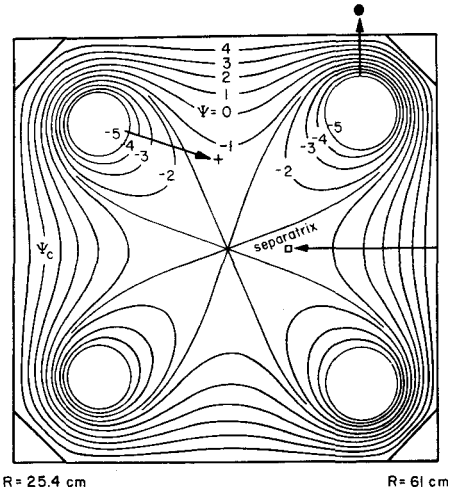

FIG. 2. Flux plot for the Wisconsin toroidal octupole. The field line at which $V'' = 0$ is labeled ψ_c. The separatrix is the field line passing through the point of zero poloidal field.

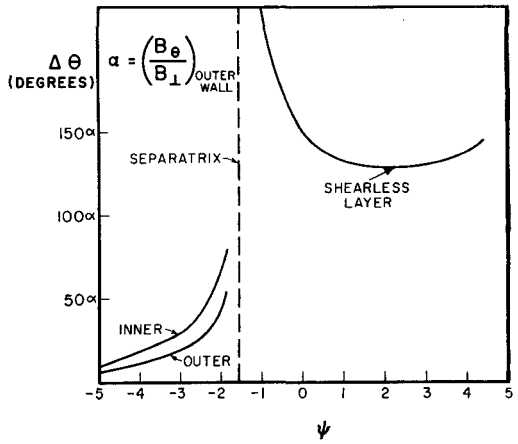

FIG. 3. The degree of progression of a field line around the major axis for each turn around the minor axis is plotted as a function of ψ. The ordinate is in units of degrees for the ratio $B_\theta/B_\perp$ at the intersection of the midplane with the outer wall. The shearless layer appears as a relative minimum.

When a toroidal field B_θ = const/R is added to the octupole field $\mathbf{B}_\perp$, the ψ lines of Fig. 2 are unchanged, but the **B** lines spiral around the current-carrying hoops. Note that the ψ line called the separatrix, shown in Fig. 2, divides the **B** lines into three classes: thus in Fig. 3 we plot $\Delta\theta$, the change in θ for which a **B** line spirals once around an inner, an outer, or all four hoops. $\Delta\theta$ scales in the quantity α, the ratio $B_\theta/B_\perp$, at the intersection of the midplane and the outer wall.

In Fig. 3 note especially the existence of a layer which has zero average shear. This is located, independently of α, at $\psi \simeq 2.25$. When there is line closure here flux tube interchange is possible, and the topology is sensitive to field errors.

With the addition of a B_θ we would expect to have shear stabilization against interchanges except (1) when finite resistivity or finite electron inertia is taken into account and (2) in the shearless layer. In the first case criteria have been given by Furth, Rosenbluth, Killeen and Coppi, and by Johnson and Greene.[14] In the limit of small plasma pressure and small resistivity Johnson and Greene predicted stability if $p'V^{**} > 0$, where

$$V^{**} = V''(\psi) - \frac{[\oint (dl/R^2B_\perp)]' \oint dl/B_\perp}{\oint (dl/R^2B_\perp) + [R_0^2B_\theta^2(R_0)]^{-1} \oint B_\perp\, dl},$$

[13] J. E. Howard, J. W. Poukey, and R. L. Willig, Bull. Am. Phys. Soc. 12, 789 (1967).

[14] J. L. Johnson and J. M. Greene, J. Nucl. Energy Pt. C9, 611 (1967); H. P. Furth, J. Killeen, M. N. Rosenbluth, and B. Coppi, in *Plasma Physics and Controlled Nuclear Fusion Research* (International Atomic Energy Agency, Vienna, 1966), Vol. I, p. 103.

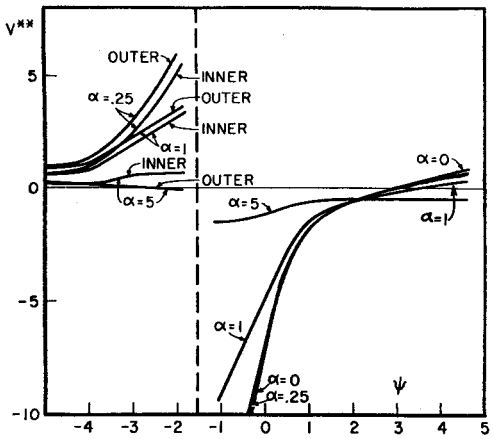

FIG. 4. The V^{**} stability criterion of Johnson and Greene (Ref. 14) is plotted against ψ for various values of $\alpha = (B_\theta/B_\perp$ at the outer wall). For $\psi > \psi_{sep}$ we have stability where V^{**} is negative. Note that the volume of the stable region increases as α increases. For $\psi > \psi_{sep}$ we have stability where the curves are positive. The $\alpha = 0$ curve corresponds to the usual V'' stability criterion.

p is the plasma pressure and the prime denotes differentiation with respect to the argument ψ. When $B_\theta = 0$ this reduces to the usual $p'V'' > 0$ stability condition. The prediction of this criterion is given in Fig. 4 for various values of α. The $\alpha = 0$ curve corresponds to V'' and shows that when the pressure is peaked on the separatrix there is stability out to $\psi \simeq 3.0$. The region near the hoops (between $\psi = -5$ and the separatrix), although not shown, has $V'' > 0$ and is stable for a positive pressure gradient. As can also be seen from Fig. 4 there is a slight increase in stable volume with increasing α. Over the experimental range of α (0–0.25) there is little change in the stability prediction.

In the second case, to study the stability of the shearless layer for infinite conductivity, define $\phi(\psi)$ as the circumferential flux (or θ — flux) inside a given ψ surface, and assume that a criterion of the form $p'(\psi)V''(\phi) > 0$ is valid. $V''(\phi)$ is found to have a constant negative value from the separatrix to the walls, similar to the high α case of Fig. 4, predicting stability even if interchange were possible. Note also that the region near the outer rod for the $\alpha = 5$ case can have a stable pressure distribution which is peaked near the rod. This is similar to the situation in the off-center levitron.

III. INJECTION AND TRANSPORT

Plasma was produced in a conical pinch gun and injected into the octupole field along a diameter of the toroid. The process by which the plasma entered the field and was trapped has been described previously.[5] The trapping process required looping

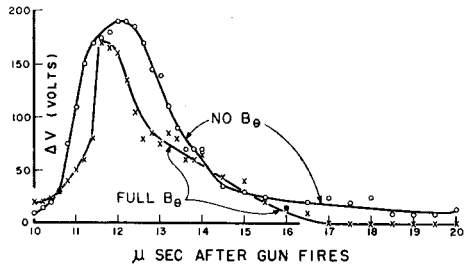

FIG. 5. Potential drop along a magnetic field line during transport compared with the potential difference between the same two points with $B_\theta = 0$. Probes were placed on each side of the injection port, 35° apart. A potential drop as large as 100 V/m was observed parallel to **B**. By 17 μsec the plasma had filled in behind the hoops and caused complete short circuiting.

field lines to short circuit the polarization fields to stop the plasma. When B_θ was added the short circuiting became less effective because of the pitch of the field lines, and plasma penetrated about 2 cm farther into the field beyond the minor axis than it did with $B_\theta = 0$.[15] For higher values of B_θ the short circuiting should become even less effective, and this type of injection might not be possible.

Without B_θ, the injected plasma splits into two clouds which $\mathbf{E}\times\mathbf{B}$ drift around the toroid by producing octupole electric fields which cause the plasma to move in a double vortex flow pattern[16] as described theoretically.[17] With B_θ, the spiraling magnetic field lines connecting the oppositely directed clouds would tend to short circuit the electric fields and to inhibit transport, unless the plasma flow were parallel to the field. The octupole electric field plots were still observed with B_θ, although they were somewhat distorted. Such a situation could exist only if there were a potential gradient parallel to the magnetic field lines. To examine this possibility, two probes were placed on the same field line on opposite sides of the injection port, and the potential difference was measured. Figure 5 shows that this potential difference was not greatly changed from that observed with $B_\theta = 0$ expect after 17 μsec when it dropped to zero.

The explanation of this behavior apparently lies in the fact that plasma fills in behind the hoops too slowly to produce a short circuit immediately. Floating double-probe density measurements showed that indeed the bulk of the plasma had moved past a given azimuth before the density behind the hoops rose appreciably.

Some plasma was observed to move parallel to

[15] J. C. Sprott, Bull. Am. Phys. Soc. **12**, 789 (1967).
[16] A. Filimonov, D. E. Lencioni, J. C. Sprott, and R. L. Willig, Bull. Am. Phys. Soc. **11**, 452 (1966).
[17] J. W. Poukey, Phys. Fluids **10**, 2253 (1967).

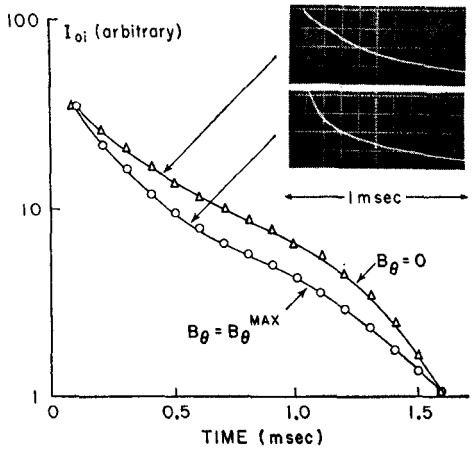

FIG. 6. Ion saturation current on the minor axis with and without the toroidal field. Note the absence of fluctuations on the oscilloscope traces and the fact that the initial decay rate is slightly greater with B_θ. The peak of the 5 msec magnetic field pulse is at 200 μsec.

the field at the point where the field was purely toroidal.[15] For higher values of B_θ, the short circuiting could be more serious, and plasma everywhere would probably move parallel to the field.

IV. DENSITY DISTRIBUTION

After the large potentials generated during filling had disappeared—that is, in about 100–200 μsec—plasma-density observations were made by measuring the saturated ion current to a single Langmuir probe 0.3 cm long and 0.3 cm in diameter.

Oscillographs of ion saturation current measured on the minor axis for cases with and without B_θ together with their semilog plots are shown in Fig. 6. Initially both signals were about the same and in neither case was there any evidence of a sudden loss of plasma or variation of density. The injection time was such that the peak of the 5 msec confining field pulse was at 200 μsec on this graph. For the first 500 μsec the decay rate was roughly

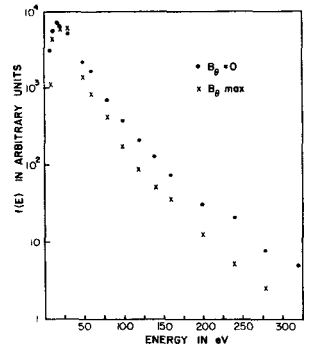

FIG. 7. Distribution function of ion energies for the zero and maximum B_θ cases.

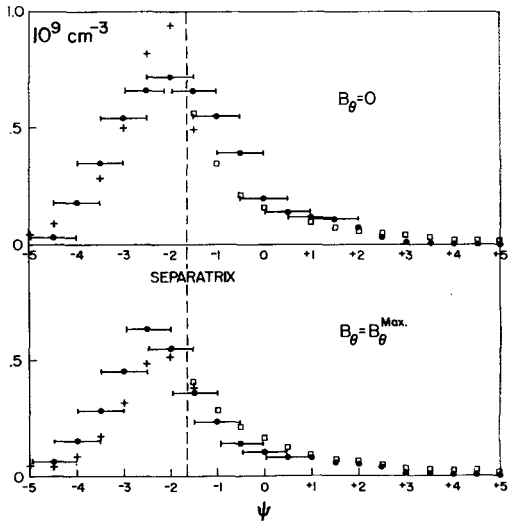

FIG. 8. The constancy of density along magnetic field lines was tested by making three scans in different regions of the octupole field as shown in Fig. 2. The density is plotted versus ψ and shows that within the accuracy of the measurements that the density is constant along ψ lines. For the scan above a hoop, the length of the probe in ψ-space is indicated by horizontal error bars. The shot-to-shot irreproducibility was taken into account by normalizing the densities against a monitor-probe reading ion saturation current on the minor axis.

30% greater for the case with a B_θ field. At approximately 1 msec both signals began to decay rapidly due to the decrease of the confining fields.

The lifetimes of ions of a particular energy were also measured during the first 500 μsec by extracting ions through a small magnetic shielding tube[18] and selecting the energy by an electrostatic analyzer. With $\alpha = 0.25$ the meanlife of 40-eV ions at the center was typically 350 μsec while with $B_\theta = 0$ it was 550 μsec.

The distribution functions of ions were also somewhat different with and without B_θ as shown in Fig. 7. There seemed to be greater loss of high-energy ions in the filling process with B_θ present.

A comparison of the density profiles measured by Langmuir probes is shown in Fig. 8. In order to test the constancy of the density along magnetic field lines, scans were made in the three different regions of the octupole field, shown in Fig. 2. The irreproducibility of the total amount of plasma, the finite probe size, and the difficulty of locating a field line led to a considerable experimental uncertainty. The irreproducibility of the total amount of plasma was taken into account by normalizing the density measurements against a monitor probe on the minor axis. For the scan above the hoop,

[18] C. W. Erickson, Rev. Sci. Instr. **37**, 1308 (1966); Bull. Am. Phys. Soc. **12**, 790 (1967).

the points are shown with a horizontal error bar indicating the length of the probe in ψ space. Note that the peak in density was displaced off the separatrix in the direction of the hoops, and that the shape of the distribution was not changed when B_θ was added.

For hydromagnetic equilibrium the density should be constant along a magnetic-field line. It was possible to place an upper limit of 25% on the difference in the magnitude of the density peak in the low- and in the high-field regions around the hoop. The density in the high-field region appeared smaller but the difference could be instrumental.

The time evolution of the density profile for the pure poloidal field is shown in Fig. 9. At approximately 1400 μsec as the plasma moved toward the walls due to the decreasing magnetic field, a reversed density gradient developed. At the same time the floating potential began to oscillate in this region of inverted density gradient. These oscillations had a frequency of about 10 kHz and an amplitude of about 0.2 V. When B_θ was added the amplitude of this oscillation decreased.

The inversion of the density gradient under all hoops and at late times might be expected to cause instability. However, in the case of the region under the hoops, the density gradient did not disappear during the experiments. Usually we apply the stability criterion $p'V'' > 0$, for stability at the edge of the plasma where p is zero. In the cases of the inverted density gradients which we are discussing, p is not zero. For $B_\theta = 0$, the condition for interchange stability including the finite pressure term can be written in the form

$$\frac{dE}{d\psi} = p'V'' + p\gamma\frac{(V'')^2}{V'},$$

$$= pV''\frac{d}{d\psi}\ln(pV'^\gamma) > 0.$$

Because of the pressure term, an inverted gradient may be stable. If we assume the temperature is a constant, then stability is determined by the slope of ln (nV'^γ) where n is the density. A plot of this function for the plasma is shown in Fig. 10. For 0.5 msec in the region to the left of the separatrix under the hoops where $V'' > 0$, we have stability. The $p'V''$ term is negative from $\psi = -2$ to the separatrix in this region of inverted density gradient under the hoops, but the pressure term dominates here and makes the plasma stable in spite of the inverted pressure gradient.

From the separatrix to ψ_c, $V'' < 0$, so again there is stability. Outside ψ_c, $V'' > 0$, so this region should be flute unstable in agreement with experimental observations.

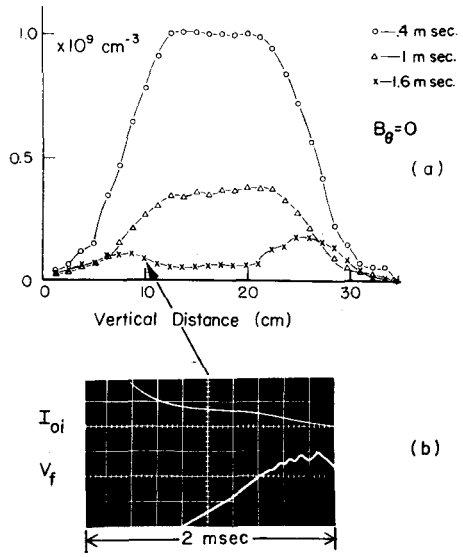

FIG. 9. (a) Density profiles on a vertical line through the minor axis showing the density inversion which develops when the magnetic field decays. (b) Ion saturation current and floating potential traces in the region of the inverted density gradient. The floating potential fluctuation has an amplitude of about 0.2 V.

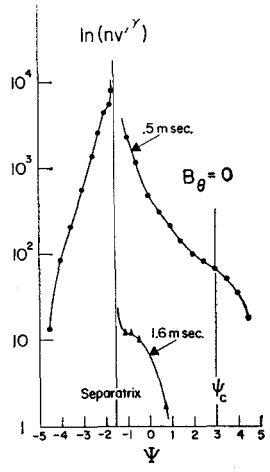

FIG. 10. The condition for interchange stability is that the quantity $\Delta E/\Delta\psi \propto V''$ $\ln(nV'^\gamma) > 0$. V'' is positive to the left of the separatrix and ψ_c and positive from ψ_c to the wall. Therefore, the plasma satisfies the interchange stability condition for all $\psi < \psi_c$. In particular it is satisfied from $\psi = -2$ to the separatrix, the region of inverted density gradient.

Also plotted in Fig. 10 are the data for the late-time density inversion at 1.6 msec mentioned previously. In this case the pressure was small and there was a region where the slope began to invert and the plasma was barely unstable. This is where the 10 kHz floating potential oscillations were seen.

Ohkawa has observed similar oscillations in this region where the density gradient inverted in his octupole.[12]

The shearless flux surface is at $\psi = 2.25$. Whenever the field lines close on themselves in this surface it becomes possible to have an interchange

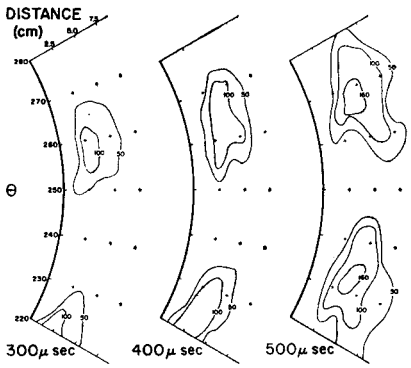

FIG. 11. Contours of equal floating potential on midplane showing the periodic structure which moves in the $+\theta$ direction. Probe resolution and shot-to-shot irreproducibility limit the picture to a rough representation of the actual contours on a given shot.

of two adjacent tubes of flux. Also the field topology becomes very sensitive to perturbations since a line can be moved a large extent in the ψ direction without becoming detuned to a perturbation at one azimuth.[19]

Measurements made with floating probes showed a helical potential structure near the shearless flux surface which spiraled around the minor axis with the same pitch as a field line. A sequence of equipotential contours in the midplane near the inner wall is shown in Fig. 11. The shearless flux surface is 3.5 cm from the wall. Because of shot-to-shot irreproducibility and finite-probe resolution these contours represent only a rough picture of the contours in a given shot. The periodic structure is evident, however, and it can also be seen that it moves in the $+\theta$ direction with a speed of $\sim 10^4$ cm/sec. The radial electric field from these contours gives an E/B rotational speed of $\sim 5 \times 10^5$ cm/sec. The motion of this structure in the θ direction caused a series of potential spikes to appear on a stationary probe at one azimuth. Also in these high potential regions the ion saturation current had high frequency (5 MHz) large amplitude ($\delta n/n \approx 100\%$) fluctuations.

A radial scan along the midplane, which cuts across a contour near the inner wall, is shown in Fig. 12. There was a reduction in density gradient across the contour while on the other side of the midplane the gradient became even larger than with no B_θ.

Since in this experiment the ratio $B_\theta/B_\perp$ decreases in time, the position of line closure moves away from the shearless surface. A sequence of radial scans of floating potential is shown in Fig. 13. As

[19] D. W. Kerst, J. Nucl. Energy Pt. **C4**, 253 (1963).

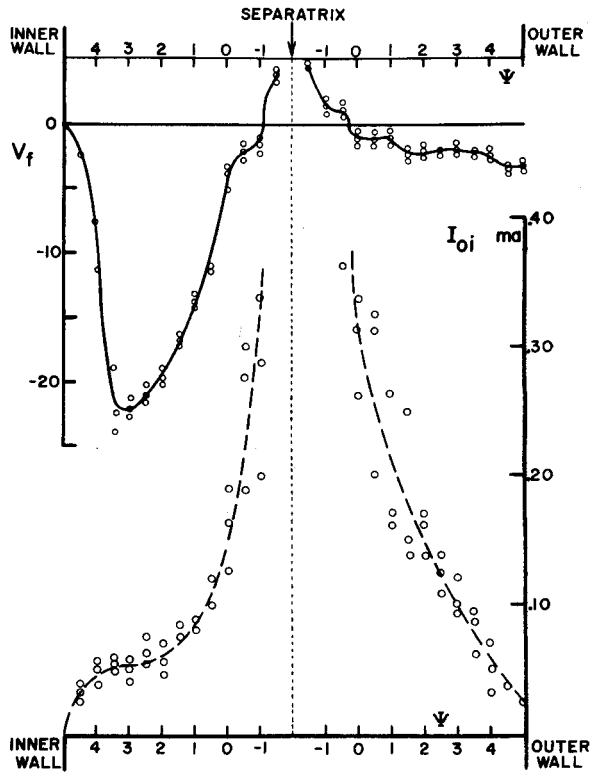

FIG. 12. Radial midplane scans of ion saturation current and floating potential showing the effects of B_θ and the potential island on the density gradient near the walls.

can be seen the potential island splits and the side peaks move away from the shearless surface. A comparison of the expected position of line closure as a function of time and the observed positions of the potential peaks are shown in Fig. 14.

The influence of magnetic-field perturbations on the lifetime of the plasma was tested by placing a permanent magnet against the vacuum tank wall. The magnet caused a 300-G perturbation to the 1000-G field at ψ_c. Various orientations of the magnet were tried with and without B_θ with no observable change in lifetime or density. The amplitude and time of appearance of the potential spikes, discussed above, were drastically changed by the field perturbation.

V. ELECTRIC FIELD FLUCTUATIONS AND DIFFUSION COEFFICIENTS

For zero B_θ, large ($\approx$3 V) fluctuations occurred outside the boundary of stability (ψ_c). The fluctuations dropped off rapidly inside the stable region.

For the finite B_θ case,[20] neglecting the island

[20] J. A. Schmidt and D. E. Lencioni, Bull. Am. Phys. Soc. **12**, 790 (1967).

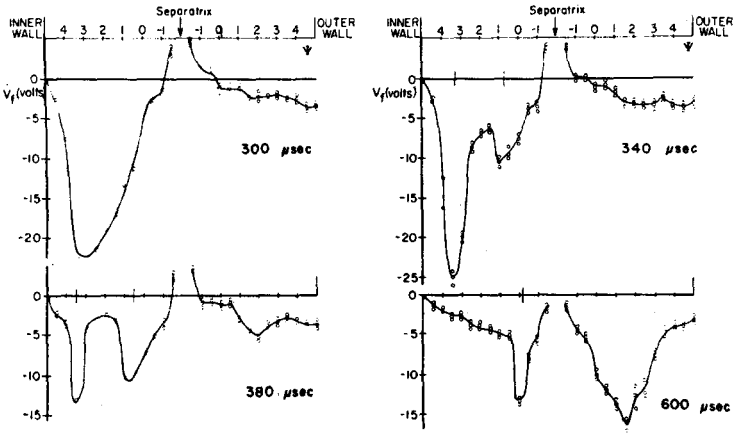

FIG. 13. Sequence of radial midplane scans of floating potential showing the splitting at the shearless surface.

structure discussed in Sec. IV, the fluctuations outside the separatrix, comprised two groups:

(a) fluctuations outside ψ_c which were reduced as B_θ increased;

(b) fluctuations on flux surfaces about 7.5 cm from the wall on the midplane which increased as B_θ increased.

The suppression of fluctuations outside ψ_c is illustrated in Fig. 15, column c, $\psi = 4.5$. For small B_θ the fluctuations were the same as they were with zero B_θ. As B_θ increased they were generally suppressed while an occasional potential deviation appeared due to moving flux islands in the shearless region.

The fluctuations appearing 7.5 cm from the wall as B_θ was added (Fig. 15, column c, $\psi = -0.5$) had a frequency in the 0.5–1.5 MHz range. They were about 0.7 V in amplitude and traveled with a phase velocity of 1.7×10^6 cm/sec in the median plane in the direction of the diamagnetic current.

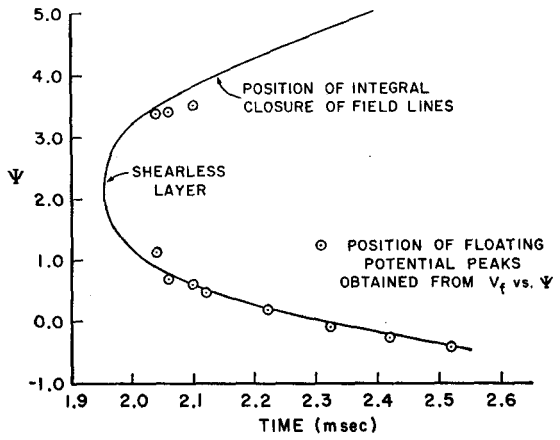

FIG. 14. A comparison of the expected position of line closure and the observed position of potential peaks.

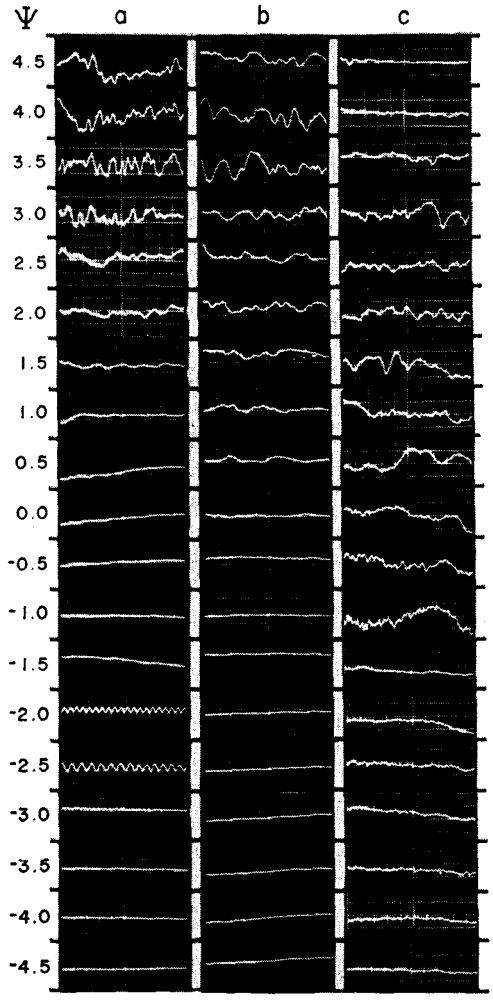

FIG. 15. Floating potential fluctuations are shown for the period from 150–250 μsec after injection. (a) Scan along the midplane from the wall to the separatrix and then along a diagonal up to a hoop for $B_\theta = 0$. The oscillations at $\psi = -2.0$ and -2.5 are an example of probe-induced fluctuations. (b) Scan across the narrow region between a hoop and the wall. Note that the probe does not induce fluctuations at $\psi = -2.0$ or -2.5. (c) Same as (a) but with B_θ added. All pictures are at 2.5 V/div.

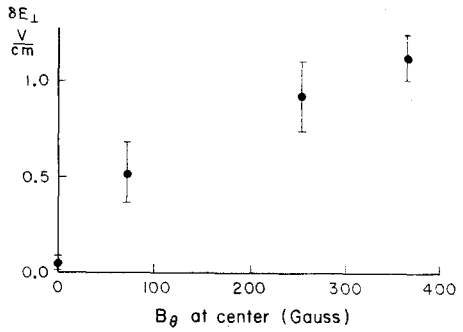

FIG. 16. Amplitude of electric field fluctuations 7.5 cm from the wall in the midplane as a function of B_θ.

The $\mathbf{E}\times\mathbf{B}/B^2$ mass motion of the plasma in this region represents at very most only 30% of this velocity. The growth of these fluctuations with increasing B_θ is illustrated in Fig. 16. In this figure the magnitude of fluctuations in electric field E_θ for a position 5 cm from the wall is plotted versus the toroidal magnetic field at the center.

The effect of the fluctuations on particle transport can be best conveyed in terms of a diffusion coefficient. An estimate of the diffusion coefficient can be obtained from measured fluctuations by applying the following analysis.

The time-average flux outward due to a fluctuating E/B drift is

$$\langle nv\rangle = \frac{1}{B}\langle(n_0 + \delta n)(E_0 + \delta E)\rangle = \frac{\langle \delta n\ \delta E\rangle}{B}.$$

Equating this to $-D\nabla n$ gives

$$D = -\frac{\langle \delta n\ \delta E\rangle}{B\nabla n}.$$

Meade[6] applied this equation for zero B_θ. He measured δE and δn and found a maximum diffusion coefficient 10^4 times smaller than the Bohm value in the central body of the plasma but rising to the Bohm value at the stability boundary at ψ_c.

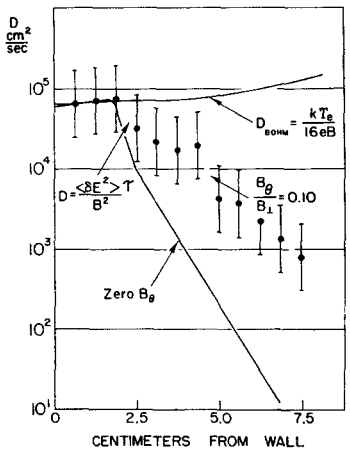

FIG. 17. The maximum diffusion coefficient on the vertical midplane for the B_θ and zero B_θ cases. The Bohm diffusion level is also given for comparison.

In the presence of an added B_θ, long wavelength potential fluctuations near the shearless layer became large enough (10 V) to affect the accuracy of the determination of δn by Langmuir probes. Consequently δn was not measured as Meade had done, but the diffusion coefficient was estimated by[21]

$$D = \frac{\delta E^2}{B^2}T.$$

In this estimate the time T during which one random step takes place was taken as one-half the period of the apparently random fluctuations.

In Fig. 17 are plotted the $B_\theta = 0$ Bohm diffusion coefficient, the zero B_θ diffusion coefficient as determined by Meade,[6] and the maximum diffusion coefficient for small B_θ ($\alpha = 0.10$). The plot was made for small B_θ to eliminate the flux islands and also to illustrate the similarity of the results of the two methods outside of ψ_c.

The evolution of the plasma density due to Bohm diffusion can be obtained if it is assumed that the flux of particles across flux surfaces is given by the equation

$$nV_\perp = -D_B\nabla_\perp n,$$

where $nV_\perp$ is the perpendicular plasma flux, n is the density and $D_B = kT_e/16eB$ is the Bohm coefficient.[6] Also, if the density is always assumed to be a function only of ψ then the following equation is obtained

$$V'\frac{\partial n}{\partial t} = \frac{kT_e}{16e}\frac{\partial}{\partial\psi}\left[G(\psi)\frac{\partial n}{\partial\psi}\right],$$

where

$$G(\psi) = \oint \frac{B_\perp R^2\,dl}{(B_\perp^2 + B_\theta^2)^{\frac{1}{2}}}.$$

Computer solutions of this equation were obtained, for $B_\theta = 0$, using the experimentally observed density distributions at 500 μsec, as the initial condition. These showed that for Bohm diffusion the peak density decayed with a meanlife of 50 μsec, a factor of about 10 less than that experimentally observed. Moreover, the actual shape of the density profile was shown to be inconsistent with that for Bohm diffusion. These results are shown in Fig. 18.

It was observed that the amplitude of the potential fluctuations decreased with increasing background gas pressure. In some cases, raising the

[21] L. Spitzer Jr., Phys. Fluids **3**, 659 (1960).

hydrogen pressure from 3×10^{-7} to 3×10^{-6} Torr decreased the amplitude of the fluctuations by a factor of 2. At slightly higher pressure some fluctuations disappeared entirely.

Since the determination of actual diffusion rates has been hampered by the presence of hangers, it would be desirable to make measurements with no hoop supports to be free from the loss of plasma to such obstacles. This type of experiment is being planned.

VI. CURRENT ALONG LINES OF FORCE

With the addition of B_θ some current parallel to field lines becomes necessary for equilibrium as is the case in stellarators. In addition, currents parallel to **B** might be caused by a nonvanishing line integral of the electric field along **B**. This can occur in the plasma region because of a time rate of change of **B** and because of a finite wall or hoop resistance. In the first case, for example, the parallel electric field at the center, where the field is purely toroidal, reached a peak value of 3.6 V/m and varied from zero to approximately 2 V/m during the time of the experiment.

The parallel current was measured with two types of directional probes, both of which consisted of two flat collecting electrodes insulated from each other so that their surfaces faced in opposite directions. In the first type of probe the electrodes were biased to collect either ion or electron saturation current and the difference in current was measured to give the net directed current for each species. In the second type of probe each electrode was used as a high impedance floating potential probe and the difference in floating potentials was measured. If a directed electron current I_D strikes one electrode, then, to first approximation, the induced difference in floating potential ΔV_f is

$$\Delta V_f = \frac{kT_e}{e} \ln (1 + I_D/I_{io}),$$

where T_e is the electron temperature, k is Boltzmann's constant, e the electronic charge and I_{io} is the random ion thermal current.

The first type of probe was used to measure a known current, namely the diamagnetic current with zero B_θ, and it gave good agreement with the predicted value needed to hold the plasma pressure.

Caution must be taken when measuring the diamagnetic current with this probe. In general the diamagnetic current through a small area in the plasma is made up of the same particles passing through this area many times. The current probe has the disadvantage of being able to count a particle only once, thereby eliminating it from the plasma. To function properly the area into which the probe is to be inserted must be such that only a small fraction of the particles pass through this area more than once in the duration of the experiment. Due to the ∇B drift across the field lines and motion along the field lines this condition can usually be met by a probe with all dimensions much smaller than a gyroradius.

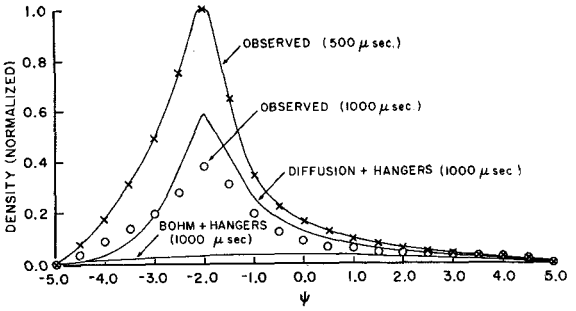

FIG. 18. The experimentally observed density profile at 500 μsec (X) was used as an initial condition in a computer program which calculated profiles at 1000 μsec for the diffusion expected from observed fluctuations + hanger losses and for Bohm diffusion + hanger losses. The experimentally observed density at 1000 μsec (0) is much larger than would be expected if Bohm diffusion were present.

When used to measure electron current both probes gave consistent results and showed that, with B_θ, there was a parallel electron current which ranged from zero at the walls to approximately 2 mA/cm^2 at the center. This should be compared with the electron thermal current of approximately 5 mA/cm^2 at the center. In the region near the shearless layer large bursts of current, approximately 1 mA/cm^2, which were comparable to the electron thermal current, were seen. These corresponded to the potential spikes discussed in Sec. IV. Consequently, the island-like configurations at the shearless layer contain currents along lines of force which produce a negative signal on floating potential probes.

VII. DISCUSSION

The influence of B_θ on various types of fluctuations observed in different regions is summarized in Table I.

In region 1 the addition of B_θ produced some shear. Also $V^{**} > 0$ as shown in Fig. 4 implied instability. The fluctuations in floating potentials decreased to about $\frac{1}{3}$ (Fig. 15), but the density fluctuations were about the same amplitude but of somewhat higher frequency.

In region 2 the average shearless region with $B_\theta \neq 0$, very large potential deviations occurred

TABLE I. Summary of the University of Wisconsin octupole experiments

	Region in octupole	Fluctuations with $B_\theta = 0$ (no shear)	Fluctuations with $B_\theta/B_\perp = 0.25$ at wall (some shear)
1.	Wall to Ψ critical $+5.0 > \Psi > 3.0$ (wall to 2.5 cm from wall)	$V_f \sim 4$ V, 100–500 kHz $\delta n/n \sim 25\%$, $\lambda \sim 3$ cm diamagnetic direction $V'' > 0$ unstable	$V_f \sim 1.5$ V-sparse $\delta n/n \sim 25\%$ higher frequency $V^{**} > 0$ unstable (shear $\Theta \sim \frac{1}{2}$)
2.	Shearless vicinity $\Psi = 2$ (4.4 cm from wall)	$E_\theta < 0.3$ V/cm	$V_f \sim kT_e \sim 10$ V on isolated flux tubes. Depends on field errors
3.	$\Psi = 0.7$ (to 7.5 cm from wall or 5 cm within plasma)	Absent $D < 10^{-4} D_{\text{BOHM}}$	$D \sim 10^{-2} D_{\text{BOHM}}$ $V_f \sim 1$ V at 5.5 cm 0.5 to 1.5 MHz, $\lambda \sim 2$ cm velocity 1.7×10^6 cm/sec in diamagnetic direction
4.	Under rods where pressure gradient inverts $\Psi = -2.5$ should be stable by: $\partial E/\partial\Psi = P'V'' + \gamma P(V'')^2/V'$	$V_f = 0.5$ V 200 – 600 kHz found only in 1 cm² area induced by probe	Absent $V_f < 0.1$ V shear $\Theta \sim \frac{1}{2}$
5.	Late time $\Psi = -1$ 10 cm from wall when pressure gradient inverts. Marginally stable according to: $\partial E/\partial\Psi = P'V'' + \gamma P(V'')^2/V'$	$V_f \sim 0.2$ V ~30 kHz	Less

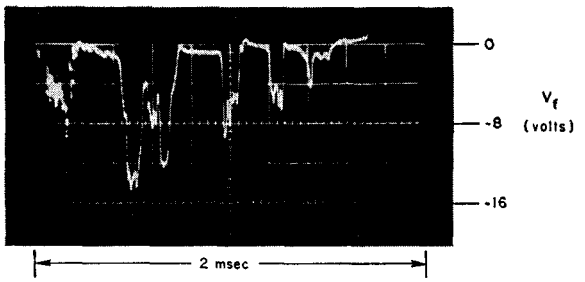

FIG. 19. Large floating potential deviations are shown as they appear in the shearless region 4 cm from the wall.

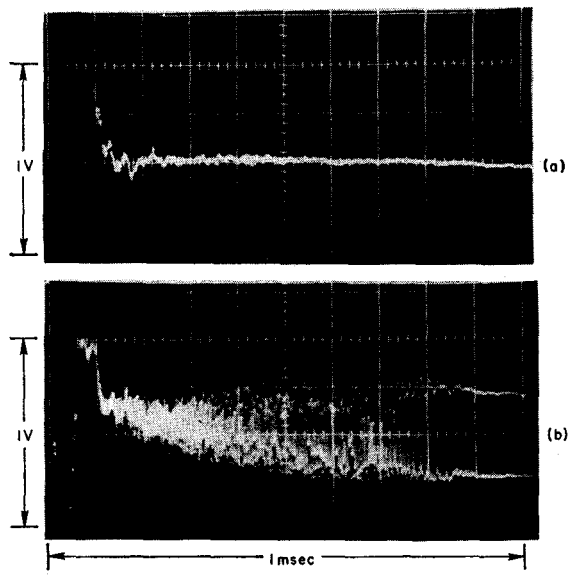

FIG. 20. Example of probe-induced fluctuations. (a) Trace taken with a 1.6-mm-diam probe in the bridge region at $\psi = -2.5$. (b) Trace taken with the same probe but with another 6.3-mm-diam probe on the same field line under the rod.

(Fig. 19), which repeated on successive fillings with plasma. A potential deviation could be followed along a tube of flux as it spiraled around the minor axis of the toroid an integral number of times.

Since this layer was shearless, large isolated flux tubes could form in the topology of the field in the presence of perturbations and at layers where the lines of force rotated an integral number of times around the minor axis so they connected with themselves.[19] The possibility then existed for an isolated flux tube to acquire a potential different from the neighboring plasma.

In region 3 the application of increasing B_θ increased fluctuations in the frequency range from 0.5–1.5 MHz (Fig. 15).

This is contrary to the observations of Ohkawa who found that a B_θ of ± 1 G eliminated fluctuations in this region.[12] However his metal wall extended into the stable region. There was no ψ critical. These fluctuations were about 0.7 V in amplitude, and the waves associated with the oscillations moved in the direction of the diamagnetic current with a speed of 1.7×10^6 cm/sec. The observations were made in the median plane where field curvature was favorable for interchange stability. These were the fluctuations that made the derived diffusion coefficient much larger with $B_\theta \neq 0$. The deviations in region 2 shown in Fig. 19, which had some influence in region 3, were ignored for this determination because these deviations of potential repeat.

In region 4 the density peaked as shown in Fig. 8. Oscillations were observed on the separatrix

side of this density peak with $B_\theta = 0$ in spite of the predicted stability. These oscillations were observed to be induced by the observing probe. The plasma was most sensitive to this inducement when the probe area per flux tube was high. For this reason a probe penetrating into the weak field midplane region caused fluctuations while a probe in the strong field bridge region did not. Figure 20 shows the potential fluctuations as seen by a probe in the bridge region with and without another probe on the same field line in the low-field region near the midplane.

In Fig. 15, columns a and b $\psi = -2.0$ and -2.5 is another illustration that a probe in the low-field region (column a) caused oscillations while one in the high field (column b) did not.

Region 5 also had a reverse density gradient at late time. The oscillations developing there were discussed in a previous section and are shown in Fig. 9(b).

It is worthy of note that the fluctuations with $B_\theta = 0$ were not lacking just because the field was zero in the center—the separatrix in the high-field region behind the hoops was also fluctuation-free, even though fluctuations were seen on each side of the separatrix in the high-field region.

It is also important to note that the addition of B_θ drastically increased fluctuations in the body of the plasma (Fig. 15); whereas, it decreased oscillations and fluctuations in relatively unimportant circumstances, i.e., outside the critical ψ line and where there was a slight density inversion.

ACKNOWLEDGMENTS

Help and valuable discussions were contributed by Professor D. W. Kerst, Professor K. R. Symon, and Professor D. M. Meade, as well as J. E. Howard. We are especially indebted to Professor H. K. Forsen for starting the work with an added B_θ. R. L. Willig contributed to some of the computer work.

The work was supported by the United States Atomic Energy Commission.

THE PHYSICS OF FLUIDS VOLUME 11, NUMBER 5 MAY 1968

Measurement of θ-Pinch End Loss Using a Gas Laser Interferometer

K. S. THOMAS
Los Alamos Scientific Laboratory, University of California
Los Alamos, New Mexico
(Received 16 October 1967)

A He–Ne gas laser interferometer has been used to make plasma density measurements outside the central plasma core of a θ-pinch plasma. At the θ-pinch coil midplane, the average plasma density is less than the sensitivity of the interferometer, that is, less than 5×10^{13} cm^{-3}. Outside the ends of the coil line densities (particles per cm of tube length) of the order of 10^{15} cm^{-1} are measured. When compared with previous data from the same θ pinch, a streaming velocity out the coil ends in the neighborhood of the ion thermal velocity is obtained.

I. INTRODUCTION

End loss is apparently the dominant loss mechanism in the present generation of large θ pinches. Measurements of the total amount of plasma present as a function of time have given plasma loss rates.[1-4] Direct measurements of plasma escaping from the ends of θ pinches have been made in several ways; direct photography,[5] pressure probes,[3] and measurement of the energy spectrum and flux of axially escaping ions.[6] This paper reports a measurement of the plasma density outside the end of the θ-pinch coil using a gas laser interferometer.

The end-loss measurements were performed on Scylla III, a 150-kJ θ pinch which has a coil 20 cm long and 10 cm in diameter, with a geometric mirror ratio of 1.3. The θ pinch was operated in the low-pressure regime (no bias field, 20-mTorr filling

[1] E. M. Little, W. E. Quinn, and G. A. Sawyer, Phys.Fluids **8**, 1168 (1965).
[2] W. E. Quinn, E. M. Little, F.L. Ribe, and G. A. Sawyer, in *Plasma Physics and Controlled Nuclear Fusion Research* (International Atomic Energy Agency, Vienna, 1966), Vol. I, p. 237.
[3] H. A. B. Bodin, T. S. Green, A. A. Newton, G. B. F. Niblett, and J. A. Reynolds, in *Plasma Physics and Controlled Nuclear Fusion Research* (International Atomic Energy Agency, Vienna 1966), Vol. I, p. 193.
[4] A. C. Kolb, W. H. Lupton, R. C. Elton, E. A. McLean, M. Swartz, M. P. Young, H. R. Griem, and E. Hintz, in *Plasma Physics and Controlled Nuclear Fusion Research* (International Atomic Energy Agency, Vienna, 1966), Vol. I. p. 261.
[5] E. A. McLean (private communication).
[6] R. L. Bingham, L. M. Goldman, and R. W. Kilb, in *Plasma Physics and Controlled Nuclear Fusion Research* (International Atomic Energy Agency, Vienna, 1966), Vol. I, p. 301.